Journal of Dental Sciences 20 (2025) 1436–1446

Available online at www.sciencedirect.com

ScienceDirect

journal homepage: www.e-jds.com

Original Article

Mechanical and biological properties of cellulose nanofibers as a dental biomaterial

Junduo Chen [a], Aobo Ma [a], Yiding Zhang [b,c], Lu Sun [a,d], Kunhua Yang [a], Juan Ramón Vanegas Sáenz [a], Guang Hong [a*]

[a] *Division for Globalization Initiative, Liaison Center for Innovative Dentistry, Tohoku University Graduate School of Dentistry, Sendai, Japan*
[b] *Department of Periodontology, Shanghai Stomatological Hospital & School of Stomatology, Fudan University, Shanghai, China*
[c] *Shanghai Key Laboratory of Craniomaxillofacial Development and Diseases, Fudan University, Shanghai, China*
[d] *Department of Prosthodontics, School of Stomatology, Dalian Medical University, Dalian, China*

Received 20 January 2025; Final revision received 4 February 2025
Available online 18 February 2025

KEYWORDS
Cellulose nanofibers;
Membranes;
Scaffolds;
Dental biomaterials

Abstract *Background/purpose:* Plant-derived cellulose nanofibers (CNF) have emerged as a promising material for biomedical applications due to their diverse and exceptional properties but application in dental research remains limited. This study aimed to use CNF as barrier membranes or scaffold materials applied in guided bone regeneration (GBR) and guided tissue regeneration (GTR).
Materials and methods: Two different thicknesses of CNF were detected by surface morphology, roughness, hydrophilicity, mechanical properties, and degradability test, and compared with GC Membrane and Ti (titanium). Additionally, the cell compatibility and cell morphology of MC3T3-E1 and HGF-1 in different groups were also studied. The alkaline phosphatase (ALP) activity of MC3T3-E1 was also examined on the 14th and 21st days.
Results: Compared to the GC membrane, CNF showed better mechanical properties but remained inferior to titanium. Soaking increased their roughness and hydrophilicity while reducing mechanical strength. CNF also exhibited degradability, and good biocompatibility, with ALP expression significantly elevated at 14 and 21 days.
Conclusion: The results of this study on various properties of CNF indicate that CNF has the potential to become a novel dental biomaterial.

* Corresponding author. Division for Globalization Initiative, Liaison Center for Innovative Dentistry, Tohoku University Graduate School of Dentistry, Seiryo-machi, Aoba-ku, Miyagi 980-8574, Japan.
E-mail address: hong.guang.d6@tohoku.ac.jp (G. Hong).

https://doi.org/10.1016/j.jds.2025.02.006

Introduction

The aging population has significantly contributed to the rise in surgical and restorative procedures in dentistry, accompanied by advancements in dental biomaterials. This includes the increasing use of implants and periodontal regeneration techniques, which often necessitate Guided Tissue/Bone Regeneration Membranes (GTR/GBR) and grafting materials. Alongside surgical techniques, the selection of these materials is crucial in determining the success and long-term prognosis of the procedure.[1]

GTR/GBR membranes are frequently employed as a therapeutic strategy to isolate periodontal defects among these grafting materials. These membranes are extensively utilized to preserve the space between the bone septum and the overlying gingival flap. Despite differences in composition and structure, the primary purpose is to prevent epithelial and connective tissue cells from migrating into regions of angiogenesis and osteogenesis, as these cells move more rapidly than bone-forming cells.[2] Moreover, compared to expanded polytetrafluoroethylene (ePTFE), a gold-standard non-resorbable membrane, biodegradable membranes have gained significant attention due to their ability to eliminate the need for secondary surgical procedures.[3—5] Resorbable membranes are classified into natural and synthetic polymers based on their material composition. Collagen membranes, such as Bio-Gide, represent the natural polymer category, while Poly(lactic-co-glycolic acid) (PLGA) most exemplifies synthetic polymers.[6] However, in current clinical practice, resorbable membranes also encounter several challenges, such as inadequate stability and rapid degradation. In a comparative analysis of PLGA membranes and collagen membranes for GBR, researchers demonstrated comparable osteogenic efficacy between the two materials at both 4-week and 8-week healing intervals. However, neither membrane exhibited ideal barrier functionality. Histological evaluation revealed extensive cellular infiltration into both PLGA and collagen membranes, accompanied by complete degradation within 24 weeks. Notably, the membrane behavior more closely resembled that of a biodegradable scaffold rather than fulfilling the intended role of a protective barrier in GBR procedures.[7] Also, relatively low mechanical strength and limited barrier function make the membrane prone to collapse. Therefore, for large-area bone defects, the use of appropriately designed scaffolds may be essential to effectively guide and promote alveolar bone regeneration.[8,9] Besides, titanium mesh exhibits excellent mechanical properties, including high strength and stiffness, which provide stable spatial support for bone regeneration. Its structural stability helps maintain graft volume during healing, while its elasticity minimizes mucosal compression.[10,11] The mechanical performance of titanium mesh correlates positively with thickness, with commonly used ranges of 0.1—0.6 mm; a thickness of 0.2 mm typically suffices for most clinical applications. Notably, studies demonstrate that larger-aperture meshes (1.2 mm) enhance bone regeneration and suppress soft tissue infiltration more effectively than smaller-aperture counterparts (0.6 mm).[12]

Scaffolds are specially designed three-dimensional biomaterials characterized by their porosity, high permeability, and fibrous structure. They facilitate cell interactions, support cell viability, and promote the deposition of extracellular matrix.[13,14] Although scaffold-free tissue engineering has gained attention, traditional biomaterial scaffolds remain the gold standard for bone regeneration. Their unmatched advantages include outstanding mechanical properties, and the precise delivery and release of critical biomolecules, making them superior to alternative materials.[15,16] In treating alveolar bone defects, customized alveolar bone augmentation can provide sufficient and precisely regenerated bone tissue, creating an optimal foundation for subsequent dental implant placement. Although titanium is the most widely used metal material in tissue engineering due to its excellent biocompatibility and mechanical properties, the disadvantages limit their application in vivo: the high elastic modulus of titanium can cause stress shielding, and the release of metallic ions through corrosion or wear, may lead to tissue loss.[17,18] Besides, non-absorbable titanium scaffolds necessitate a second removal operation, which increases the risk of infection and patient discomfort.[19]

CNF are environmentally friendly materials derived from natural sources, known for their outstanding mechanical strength, excellent biocompatibility, versatile surface chemistry, and unique optical characteristics.[20,21] Due to the unique structure and morphology of CNF, which can serve as a high-tech, sustainable, and partial substitute for fossil resource-based polymers.[22] As a type of nanofiber, CNF also offers advantages for oral tissue repair due to its high surface area-to-volume ratio and microporous structure. Additionally, it has the potential to promote cell adhesion and proliferation.[23,24]

In this study, CNF materials were fabricated into samples of two kinds of thicknesses (0.2 mm and 1 mm), which compared with common commercial dental materials, GC Membrane, and titanium. We hypothesize that CNF can serve as substitutes for membranes and scaffold biomaterials. The primary aim of this study is to explore the potential of CNF as a biomaterial and evaluate its applicability in dental applications.

Materials and methods

Specimen preparation

Two types of CNF samples (Chuetsu Pulp & Paper, Toyama, Japan), CNF-1 (1 mm in thickness) and CNF-0.2 (0.2 mm in thickness) were created by dehydrating an aqueous solution of Nanoforest (Chuetsu Pulp & Paper) after a pressurizing and drying process. This process enhances the physical characteristics of CNF by increasing the degree of dehydration. Commercially produced titanium plates (Grade 2, ASTM F67 unalloyed Ti) were purchased by Nippon Steel Corporation. GC Membrane (300 μm thick), a synthetic polymer composed of PLGA, was purchased by GC Corporation.

Materials treatment

Due to the water absorption properties of CNF, it is essential to exclude its effect on mechanical properties and subsequent biological experiments. In this experiment, the various types of CNF were immersed in PBS solution (Phosphate-buffered saline; Thermo Fisher Scientific, Inc., Waltham, Manassas, USA) and left to stand for 3 day at 37 °C to allow the material to fully absorb the PBS solution (Thermo Fisher Scientific, Inc.). The treated materials were named CNF—1S (1 mm thickness, soaked) and CNF-0.2S (0.2 mm thickness, soaked) respectively. To exclude the effect of the PBS solution (Thermo Fisher Scientific, Inc.) immersion process on the material, pure titanium and GC Membrane of the same specifications were subjected to the same immersion treatment, used as control groups, and designated as Ti—S and GC Membrane-S. The surface of pure titanium was ground and polished to achieve conditions similar to clinical use. All samples were cleaned using ultrasonic baths of distilled water.

Surface morphology and roughness

The soaked samples were dried by freeze-drying method before being subjected to surface morphology observations, which need to be dehydrated with ethanol solutions for 30min and then placed in fresh t-butyl alcohol (FUJIFILM Wako Pure Chemical Corporation, Osaka, Japan) for 20 min and repeated three times. The samples were placed in metal containers, with 50 μL of t-butyl alcohol added to the surface of each sample and then frozen at −20 °C for 2 h. The frozen containers with the samples were placed in a freeze-drying unit (JFD-320, JEOL, Tokyo, Japan), where the remaining water in the samples was replaced with t-butyl alcohol under freezing conditions and dried through t-butyl alcohol sublimation. All samples were coated with platinum using an automatic fine coater (JFC-1600, JEOL) to enhance conductivity. The samples were then observed using a scanning electron microscope (JSM-6390LA, JEOL) at 10 KV. The structure roughness and three-dimensional image were estimated from a laser scanning roughness (Shimadzu SFT-4500, Kyoto, Japan).

Surface wettability

The hydrophilic property of all samples was determined using a portable contact angle meter (PCA-1, KYOWA, Saitama, Japan). The excess solution was gently wiped from the surface of the soaked sample using lint-free paper before the test. An auto pipette and a goniometer were employed to ensure uniformity of the distilled water droplet volume (2 μl). Images were analyzed with FAMAS software for 1 s after the water dropped.

Shore A hardness test

The Shore A Hardness of all samples was measured to evaluate the surface hardness. Experiments were conducted on Ti, CNF-1, and CNF—1S. All experimental groups consisted of samples measuring 10 mm × 10 mm. The measurements were taken using a Shore A Hardness tester (Durometer Type A, Teclock Co., Nagano, Japan). Five distinct places on the same surface, separated by 2 mm, were used to replicate each type of hardness measurement. For that specific test, the sample's true hardness value was determined by averaging these five values (n = 5).

Flexural strength

Flexural strength was tested via a three-point bending method. Four groups of Ti, CNF-1, and CNF—1S, measuring 10 mm × 60 mm, were fixed on the fixture of a universal testing machine (Instron model 5565, Instron Corp, Canton, MA, USA) with a span of 50 mm. The experiments were conducted at a constant rate of 1 mm/min until the samples fractured or the applied force stabilized. For that specific test, the sample's flexural strength value was determined by averaging these five values (n = 5).

Tensile test

Tensile tests were used to evaluate the elastic modulus of the samples. Experiments were conducted on GC Membrane, CNF-0.2, and CNF-0.2S samples, each measuring 10 mm × 30 mm, which were secured in the grips of a universal testing machine with a span of 10 mm. All experiments were conducted at a constant rate of 5 mm/min until the samples fractured. For that specific test, the sample's tensile test value was determined by averaging these five values (n = 5).

Degradability and water absorption

Gravimetric analysis was used to determine the initial weight, pre-drying weight after the experiment, and post-drying weight after the experiment of the cellulose nanofibers to evaluate their biodegradability and water absorption. The initial weight of the samples (W0) was recorded. All samples were then incubated for 1, 2, and 4 weeks at 37 °C in 5 mL of PBS (Thermo Fisher Scientific, Inc.). Fresh 5 mL were added to the PBS (Thermo Fisher Scientific, Inc.) each week. At the designated test time point, the sample was removed from the solution, and excess liquid was gently wiped from its surface using lint-free paper. After the samples were placed in a drying oven and removed after three days, the current weight (W) was measured. The weight ratio between the initial weight (W0) and the current weight (W) of the degraded membrane is calculated according to the formula: Weight ratio (%) = W/W0 x 100. Three times experiment was repeated at each time point.

Cell culture

MC3T3-E1 mouse calvaria-derived cell line (CRL-2594, ATCC, Manassas, VA, USA) and Human gingival fibroblast cells (HGF-1, CRL46 2014, ATCC) were used to evaluate the biocompatibility. MC3T3-E1 was cultivated using the Minimum Essential Medium, Alpha Modification (α-MEM, Nacalai Tesque, Kyoto, Japan), which included 10 % fetal bovine serum (Thermo Fisher Scientific Inc.) and 1 % Penicillin-Streptomycin Solution (Nacalai Tesque), in an incubator with 5 % CO_2 at 37 °C. HGF-1 was produced in Dulbecco's

Modified Eagle Medium (D-MEM, Nacalai Tesque), which included 10 % fetal bovine serum and 1 % Penicillin-Streptomycin Solution, in an incubator with 5 % CO_2 at 37 °C.

Cell morphology

To detect cell morphology on various samples, 10,000 cells/cm^2 of MC3T3-E1 and HGF-1 were seeded on different samples and cultures for 24 h, respectively. All samples were rinsed twice with PBS (Thermo Fisher Scientific, Inc.) and then fixed at 4° in 2.5 % glutaraldehyde solution overnight after the culture time point. The fixed cells were then rinsed 3 times with PBS (Thermo Fisher Scientific, Inc.) for 10 min and dehydrated with ethanol solutions (60 %, 70 %, 80 %, 90 %, 95 %, and 100 % v/v). The samples were then placed in fresh t-butyl alcohol (FUJIFILM Wako Pure Chemical Corporation) for 30 min. The following steps were the same as the surface morphology test.

Cell proliferation

Cell proliferation of MC3T3-E1 and HGF-1 in different samples was detected by Cell counting kit-8 (CCK-8, Dojindo, Kumamoto, Japan). The samples of GC Membrane, CNF-0.2S, Ti, and CNF–1S were placed in a 24-well culture plate, and 1 mL of MC3T3-E1 cell suspension with a density of 1×10^4 cells/ml was added to each sample and cultured for 1, 4, and 7 days. At each collection time point, 550 μl of a solution consisting of the CCK-8 and culture medium in a 1:10 ratio was added to each sample and incubated for an additional 2 h. Then, 100 μl of the resulting solution was transferred to a 96-well plate and absorbance was measured at a wavelength of 450 nm.

Cell differentiation

The cell differentiation only for MC3T3-E1 will be tested by an alkaline phosphatase kit (ALP-kit, FUJIFILM Wako Pure Chemical Corporation). The samples of Ti, CNF–1S, GC Membrane, and CNF-0.2S were placed in a 24-well culture plate, and 1 mL of MC3T3-E1 suspension with a density of 1×10^4 cells/ml was added to each sample. The samples were cultured for 14 and 21 days.

Statistical analysis

All experiments were repeated three times, and the data were expressed as mean standard deviation (SD). Comparing more than two groups, a one-way analysis of variance (ANOVA) was utilized, and when comparing only two groups, the t-test was utilized. At $P < 0.05$, a significant difference was considered to exist.

Results

Surface morphology and roughness

The surface morphology of four materials before and after immersion was examined using SEM at 100x and 500x magnifications. In Fig. 1, compared to the smooth surface of pure titanium, the GC membrane group exhibited a typical porous structure. The CNF group showed fibrous structures, which were more pronounced in the CNF-0.2 group due to preparation differences, while the CNF-1 group had a smoother surface due to compression. After immersion and drying, the GC Membrane-S and Ti–S groups showed no significant morphological changes compared to the original samples, except for a slight deposition of t-butyl alcohol crystals. In contrast, the fibrous structures on the surfaces of the CNF-0.2S group and CNF–1S group exhibited noticeable swelling, likely due to the inherent water absorption properties of the materials.

A laser microscope at 500x magnification was used to observe surface roughness, construct 3D images, and measure the mean height (Rc) and arithmetic mean height

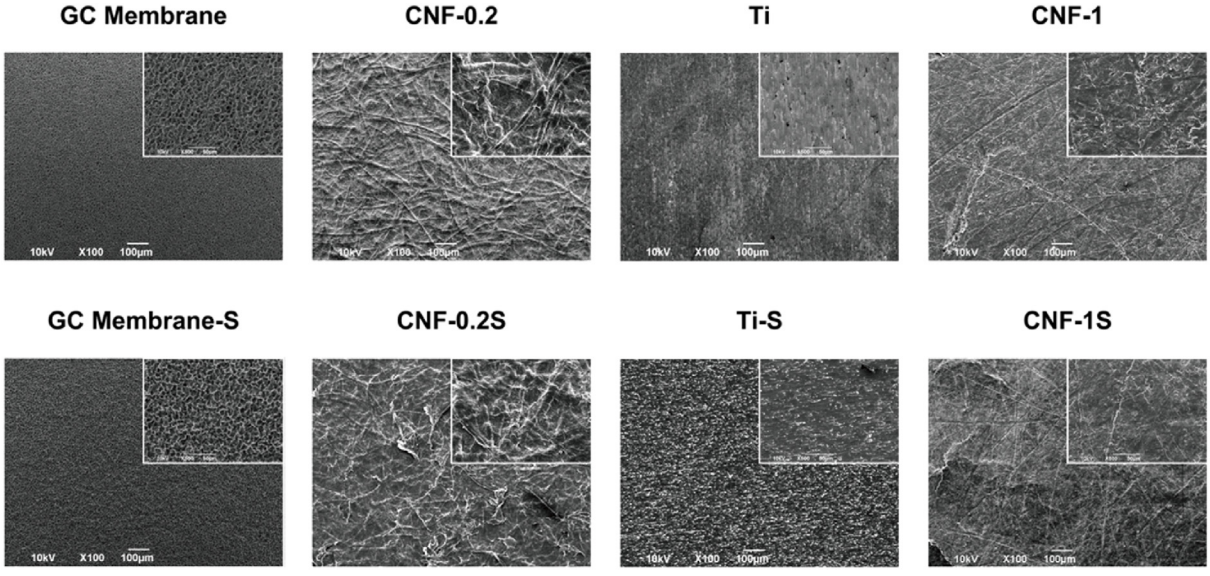

Figure 1 Different surface morphology images were detected by SEM, respectively (100 ×, scale bar = 100 μm). Insets of images were magnified SEM graphs (500 ×, scale bar = 50 μm).

(Ra) values. Fig. 2 shows trends consistent with SEM results, with CNF displaying typical fibrous structures, more pronounced in the CNF-0.2 group than in CNF-1. Fig. 3 and Table 1 indicate a significant increase in surface roughness after immersion and drying only in all CNF groups. Due to the lack of significant changes and the absence of clinical processing requirements, the GC membrane-S and Ti—S groups were excluded from further experiments.

Wettability

As shown in Fig. 4, the contact angles of all groups were lower than those of the GC membrane group. The CNF-1 group exhibited values like the Ti group, while the CNF-0.2 group demonstrated smaller contact angles than the CNF-1 group. Hydrophilicity increased across all CNF groups following treatment.

Mechanical strength

This study explored the CNF as a novel biomaterial for dental applications, particularly dental membranes and scaffolds. The experimental design included two distinct material groups: (1) the membrane group (GC membrane, CNF-0.2, and CNF-0.2S) and (2) the scaffold group (Ti, CNF-1, and CNF—1S). Mechanical characterization methods were selected based on the inherent properties of each material type. For flexible membranes, tensile testing was prioritized, as conventional hardness measurements and three-point bending tests are unsuitable for thin, pliable materials. In contrast, for rigid scaffolds, mechanical performance was assessed using Shore A hardness measurements and three-point bending tests, which better capture load-bearing capacity. This approach ensured that mechanical assessments were physiologically relevant and aligned with the intended clinical applications of each material. As shown in Fig. 5A, the CNF-0.2 group exhibits significantly higher tensile strength than the GC membrane group, though the elastic modulus and tensile strength of the CNF-0.2S group are notably lower. In Fig. 5B, the surface hardness of the CNF-1 group exceeds that of pure titanium, and while the CNF—1S group shows a slight reduction, it remains comparable to pure titanium. Fig. 5C shows a significant difference between the groups, with titanium having almost three times the flexural strength of the CNF-1 group. The flexural strength of the CNF—1S group is lower than the CNF-1 group but remains higher than the GC membrane group.

Degradability and water absorption

As shown in Fig. 6, the biodegradation of the CNF was evaluated by weight loss and weight change after soaking CNF in PBS solution (Thermo Fisher Scientific, Inc.). The

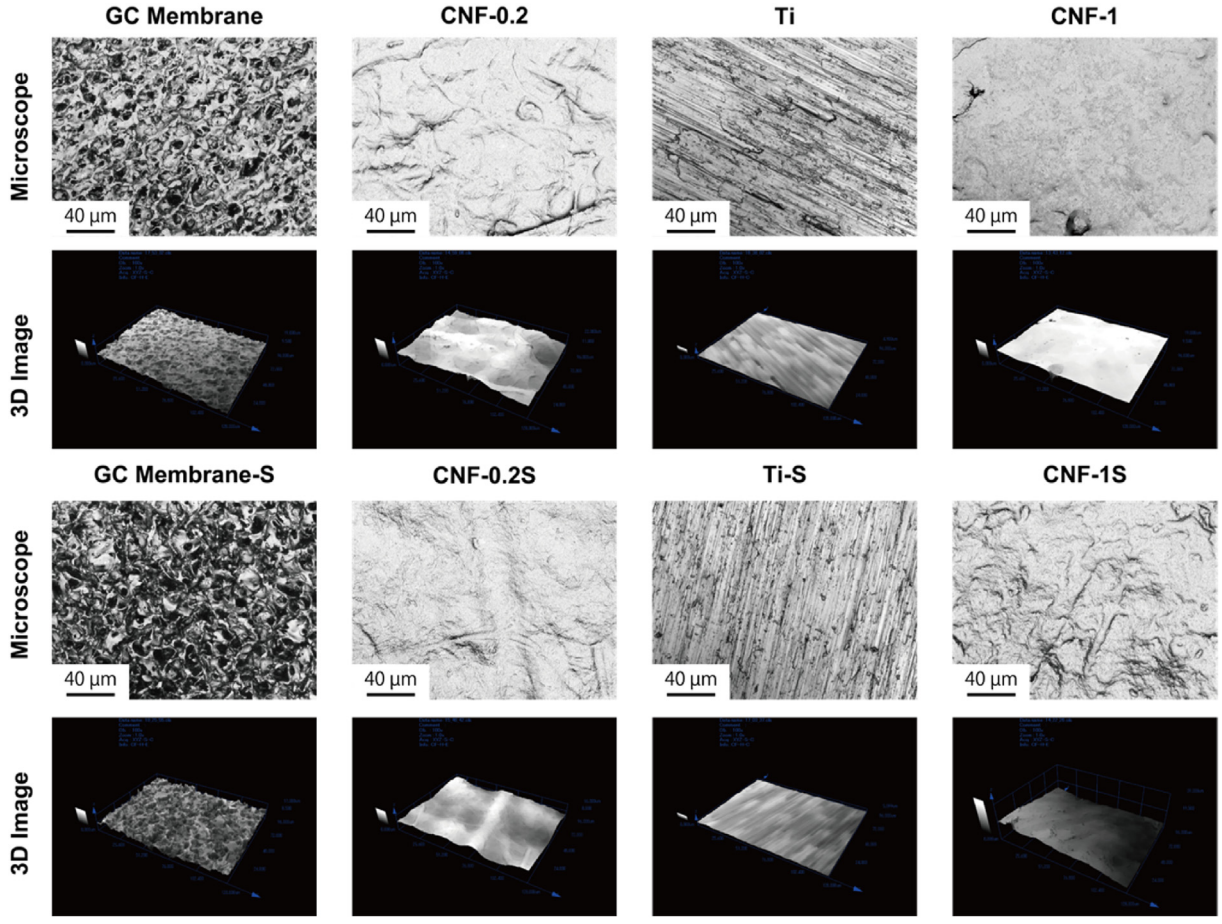

Figure 2 Laser microscope images and 3D roughness images.

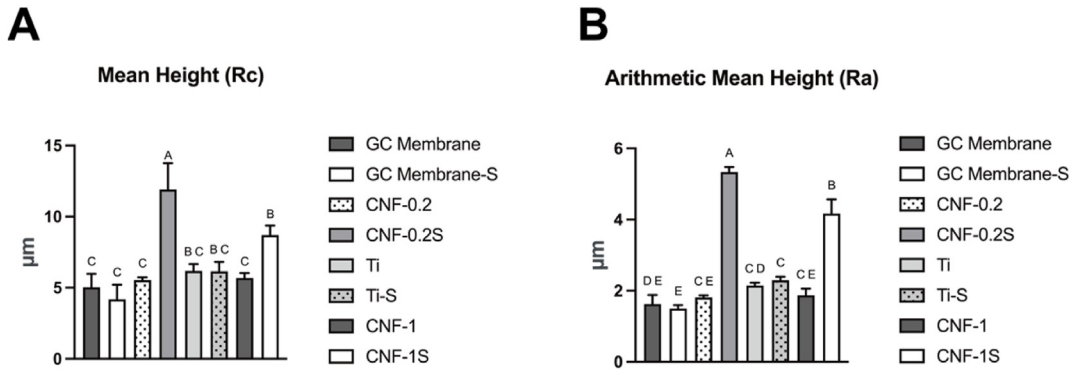

Figure 3 Roughness value of different samples. (A) Mean height valve (Rc); (B)Arithmetic mean height (Ra). Different lowercase letters indicate statistically significant differences between groups ($P < 0.05$). Data are presented as mean ± SD, with n = 3 replicates for each group.

Table 1 Rc and Ra results of different samples.

	GC Membrane	GC Membrane-S	CNF-0.2	CNF-0.2S	Ti	Ti–S	CNF-1	CNF–1S
Rc (μm)	5.04 ± 0.94	4.18 ± 1.03	5.53 ± 0.2	11.91 ± 1.85	6.18 ± 0.49	6.15 ± 0.66	5.68 ± 0.36	8.7 ± 0.67
Ra (μm)	1.63 ± 0.25	1.49 ± 0.1	1.81 ± 0.07	5.33 ± 0.14	2.15 ± 0.08	2.29 ± 0.1	1.87 ± 0.19	4.17 ± 0.4

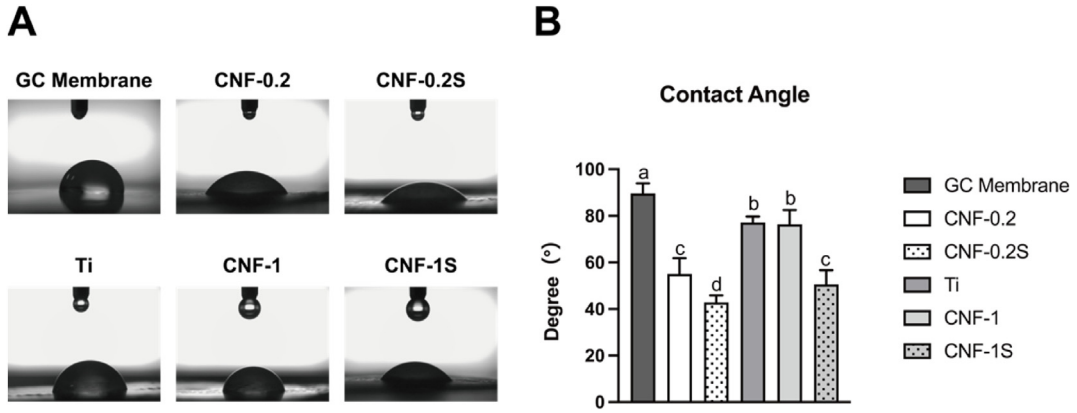

Figure 4 Contact angles of various samples. (A) Images of contact angles on different surfaces; (B) Contact angle values of different surfaces. Data are expressed as mean ± SD, n = 3 replicates per group. Different lowercase letters indicate statistically significant differences between groups ($P < 0.05$). Data are presented as mean ± SD, with n = 3 replicates for each group.

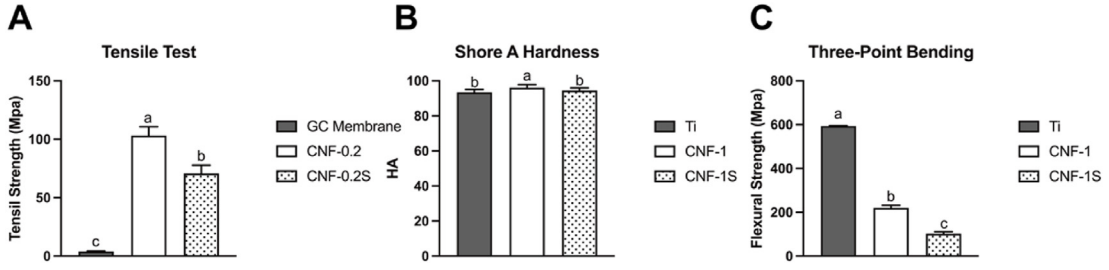

Figure 5 Mechanical strength of different samples. (A) Tensile strength; (B) Surface hardness; (C) Flexural strength. Data are expressed as mean ± SD, n = 5 replicates per group. Different lowercase letters indicate statistically significant differences between groups ($P < 0.05$).

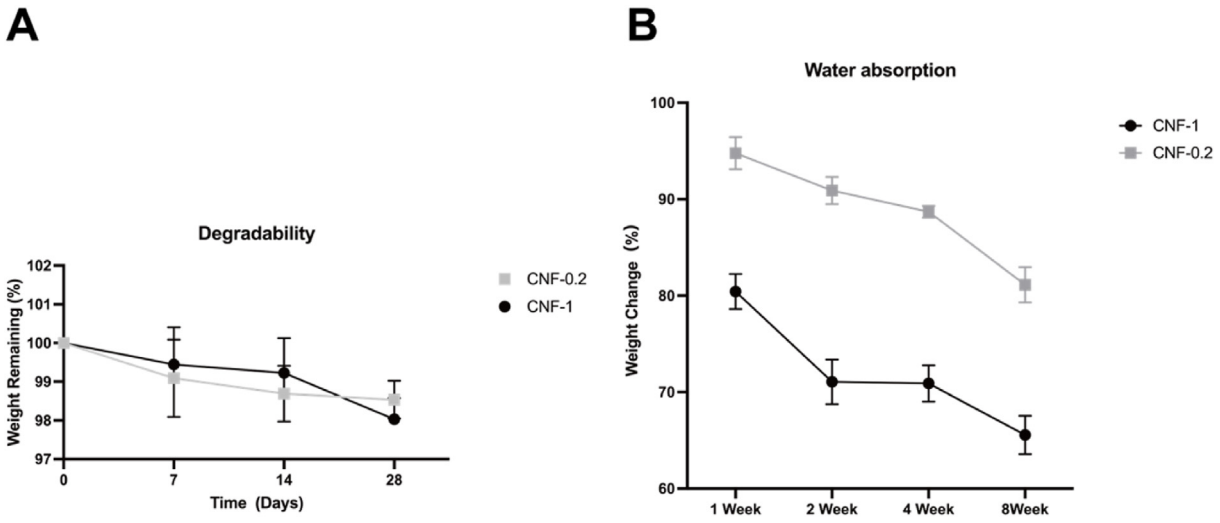

Figure 6 Degradation and water absorption analysis. (A) Degradability line graph of CNF; (B) Water absorption line graph of CNF.

in vitro biodegradation tests conducted at week four demonstrated a slight reduction in the weight of all nanofibers, suggesting the initiation of degradation, albeit at a slow rate, with a maximum degradation rate is no more than 4 %. Due to the minimal rate of degradation, the effect of degradation can be excluded from the water absorption test. The absorbency of the samples decreases over time. Meanwhile, the water absorption of the CNF-1 group was generally lower than that of the CNF-0.2 group.

Cell morphology

In Fig. 7, MC3T3-E1 cells HGF-1 were incubated on all sample surfaces for 24 h and detected early cell adhesion by SEM in 100X and 500X magnification. In the GC membrane and Ti groups, MC3T3-E1 and HGF-1 cells exhibited a typical fibroblast-like morphology. Despite being seeded at the same density, HGF-1 cells were relatively fewer in number and displayed larger surface areas than MC3T3-E1 cells after 24 h of culture, likely due to differences between cell lines and primary cells. In contrast, in the CNF-0.2S and CNF—1S groups, cells were scarcely observed, possibly due to material deformation during preparation significantly affecting cell adhesion.

Biocompatibility

To evaluate the impact of the immersion experiment on the biocompatibility of CNF materials, MC3T3-E1 cells were seeded on the materials before and after immersion, and cell proliferation was assessed on days 1, 4, and 7. As shown in Fig. 8, while the proliferation of CNF materials did not reach the level of the control group, the cell proliferation capacity significantly improved after immersion at all time points.

The results of the cell proliferation experiments are presented in Fig. 9. On day 7, MC3T3-E1 proliferation on CNF-0.2S was lower than that on the GC Membrane group,

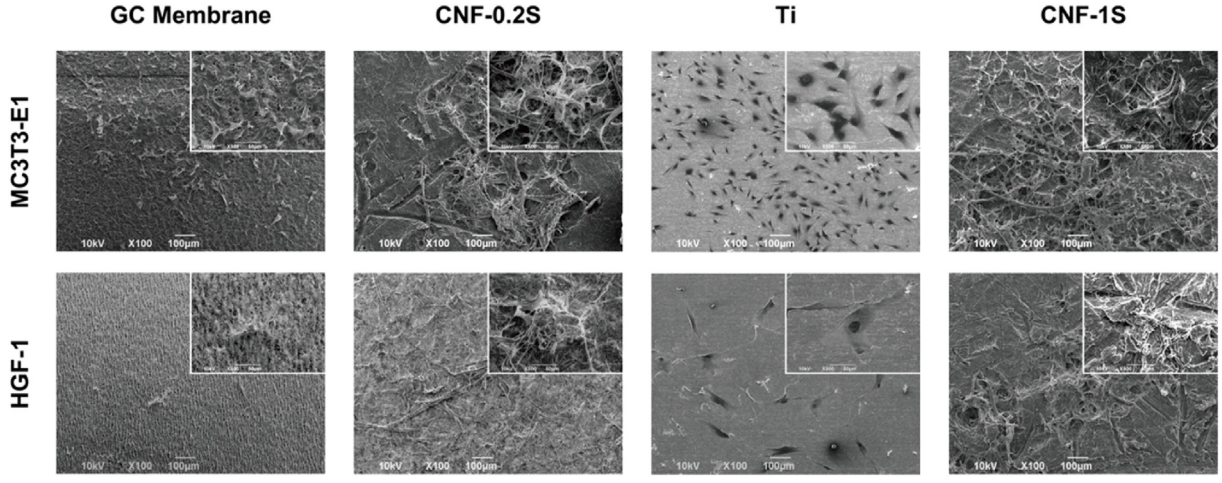

Figure 7 Morphological images of MC3T3-E1 and HGF-1 were obtained by SEM, respectively (100 × , scale bar = 100 μm). Insets of images were magnified SEM graphs (500 × , scale bar = 50 μm).

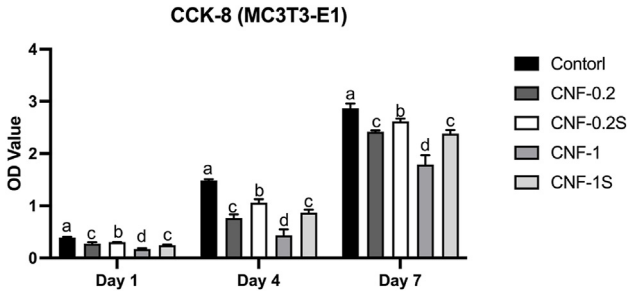

Figure 8 Cell proliferation results before and after CNF immersion treated. MC3T3-E1 cells were cultured on different surfaces for 1, 4, and 7 days. Different lowercase letters indicate statistically significant differences between groups ($P < 0.05$). Data are presented as mean ± SD, with n = 3 replicates for each group.

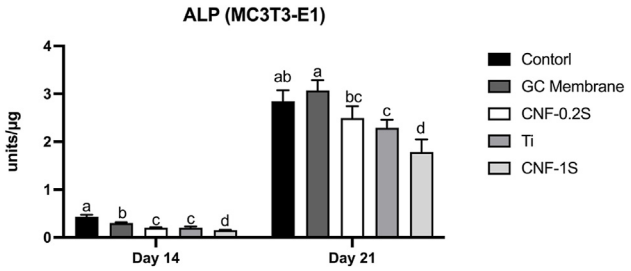

Figure 10 Cell differentiation results of different samples. MC3T3-E1 cells were cultured on different surfaces for 14 days and 21 days. Different lowercase letters indicate statistically significant differences between groups ($P < 0.05$). Data are presented as mean ± SD, with n = 3 replicates for each group.

while CNF−1S showed lower proliferation compared to the Ti group. Additionally, proliferation on CNF-0.2S was higher than on CNF−1S. For HGF-1, proliferation on CNF-0.2S showed a significant difference compared to the GC Membrane group, whereas proliferation on CNF−1S was lower than on titanium. Notably, proliferation on CNF-0.2S was higher than on CNF−1S and showed no significant difference compared to the Ti group.

The ALP activity is shown in Fig. 10. Over the culture period from 14 to 21 days, the ALP activity increased in all experimental groups. On the 21st day, the activity of the CNF-0.2S group was lower than that of the GC Membrane group. The activities of both the CNF-0.2S group and the CNF−1S group were significantly higher than that of titanium. Additionally, the activity of the CNF-0.2S group was higher than that of the CNF−1S group.

Discussion

CNF, a subset of nanocellulose, including nanoscale cellulose and crystalline nanocellulose (CNC), are micron-length fibers with diameters ranging from 20 to 40 nm. In recent years, the potential applications of nanocellulose have been extensively explored, particularly in pharmaceutical and biomedical applications, but knowledge about plant-derived CNF remains limited. This study aims to explore the application of wood-derived CNF in dental biomaterials. Mechanical and biological properties of CNF as membranes and scaffolds compared with commercially available materials currently in use were evaluated. CNF is a promising alternative for dental biomaterial applications, including guided tissue regeneration membranes and tissue engineering scaffolds, based on its unique combination of biological compatibility, structural robustness, and economic viability. The material's exceptional biocompatibility, enzymatic biodegradation profile, and non-cytotoxic nature, coupled with remarkable tensile strength and cost-effectiveness, positions it as a competitive candidate for clinical translation. We employed a commercially established PLGA membrane (GC membrane) for systematic evaluation as the benchmark control. Pure titanium, as a commonly used commercial metal, is widely employed in implant materials due to its excellent biocompatibility, which serves as a positive control for CNF as a high-strength scaffold material.

Substrate materials supporting cell viability can modulate cellular phenotypes and functions by modifying surface topography, thereby impacting various cellular activities and behaviors, especially micro/nano size. In Fig. 1, the obvious fibrous structure of CNF is observed through SEM. Compared to the 1 mm-thick membrane, the 0.2 mm-thick CNF membrane demonstrates a more prominent surface fibrous structure, resulting in a non-uniform morphology and potentially higher surface roughness. This phenomenon may be attributed to the unique pressure application during the fabrication process, which influences the morphological characteristics of CNF membranes with varying thicknesses.

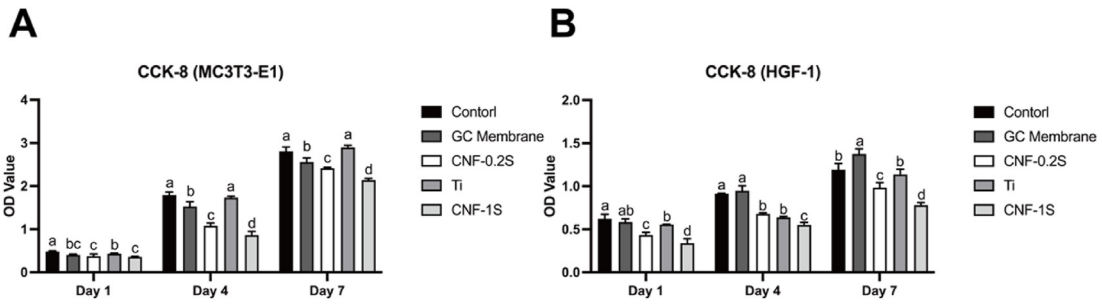

Figure 9 Cell proliferation results of different samples. (A) MC3T3-E1 cells were cultured on different surfaces for 1, 4, and 7 days; (B)HGF-1 cells were cultured on different surfaces for 1, 4, and 7 days. Different lowercase letters indicate statistically significant differences between groups ($P < 0.05$).

Furthermore, compared to the untreated material, the fibrous surface structure of CNF membranes becomes more significant after immersion treatment and subsequent drying. The 3D images in Fig. 2, combined with the roughness parameters Ra and Rc presented in Fig. 3 and Table 1, demonstrate a significant swelling and enlargement of the CNF fibrous structures after immersion and drying, with marked differences compared to the original material.

Moreover, the hydrophilic ability of CNF imparts softness to the fibers, leading to a relatively loose and flexible surface structure.[25] However, the drying process may significantly impact the material's morphology and potentially disrupt surface-adherent components, including cellular structures. As shown in Fig. 7, the unavoidable drying process during cell electron microscopy experiments can cause material deformation, potentially resulting in the detachment of cells adhered to the surface. Therefore, preserving cellular structures on the material's surface after drying warrants further investigation, while a comparison between Figs. 1 and 7 reveals significant differences between the original materials and the cell-cultured substrate materials.

Alterations in hydrophilicity can significantly affect the surface adsorption of adhesive proteins and cell stiffness. Thus, assessing hydrophilicity provides a critical parameter for evaluating material properties and predicting subsequent cellular biological responses. From the contact angle experiment shown in Fig. 4, following immersion treatment and subsequent drying, a reduction in contact angle was observed in all CNF membranes. This reduction was notably more pronounced in the 0.2 mm-thick CNF membranes compared to the 1 mm-thick ones, potentially attributed to the enhanced prominence of their surface fibrous structure post-treatment. These findings are consistent with the morphological characteristics observed in the SEM analysis.[26] Furthermore, related experiments have demonstrated that materials with moderate water contact angles (ranging from 30° to 60°) facilitate the adsorption of serum proteins, ultimately promoting cell adhesion.[27] Notably, the contact angles of CNF membranes fall within this favorable range.

In mechanical experiments, surface hardness and flexural strength are important parameters for evaluating scaffold performance, as they affect the stability, durability, and overall mechanical properties of the scaffold.[28] Fig. 5B shows that the surface hardness of CNF-1 is greater than that of titanium. Even though the physical properties of CNF−1S are somewhat reduced due to the hydrophilicity of CNF, the surface hardness of CNF−1S still shows no significant difference compared to titanium. In the three-point bending test, as shown in Fig. 5C, CNF-1 exhibits a significant difference in flexural strength compared to titanium. Moreover, the flexural strength of CNF−1S is further reduced compared to CNF-1. This indicates that while CNF can achieve similar surface hardness to titanium, their flexural strength is still insufficient, with a limited stress range. When comparing membranes, as shown in Fig. 5A, the tensile test demonstrates that CNF-0.2 has a significant advantage in elastic modulus over GC Membrane. Even though the strength of CNF-0.2S is reduced compared to CNF-0.2, it still shows a significant advantage over GC Membrane. This indicates that CNF membranes can maintain a stable structure and function in tissue repair, resisting excessive deformation or rupture. This is crucial for ensuring the barrier function and long-term support of the membrane.[29] In the degradation test, Fig. 6 indicate that neither a 1 mm thickness nor a 0.2 mm thickness alters the inherent properties of CNF, which exhibits low degradability. Studies have shown that tree-extracted CNF exhibits no degradation effects at temperatures up to 100 °C.[30]

One of the key considerations for membrane and scaffold materials in tissue engineering is their ability to support cell adhesion and migration. Recently, Takata et al. investigated osteoblast migration on various membranes used for guided bone regeneration, including bovine type I collagen, PLGA, expanded polytetrafluoroethylene (e-PTFE) and cellulose acetate-cellulose nitrate copolymers. Their results indicated that the PLGA membranes demonstrated the most superior cell migration. However, cellulose-containing Millipore membranes outperformed collagen membranes in supporting cell migration. This study underscores the promising potential of cellulose-based membranes for future research and applications.[31]

During material characterization, the morphology of CNF materials was changed due to water absorption, which needs further investigation to determine the impact of such deformations on cell adhesion and growth. Comparative CCK-8 assay analysis conducted before and after immersion revealed a significant reduction in cell proliferation capacity on untreated CNF surfaces. This effect was more obvious in the thicker CNF-1 samples. This phenomenon may contribute to the expansion of the material which may generate mechanical stress on adhered cells, potentially influencing their morphology and functional behavior. Excessive expansion could induce cellular stress or detachment, thereby impairing cellular activity and hindering tissue integration.[32]

In the research on oral membrane and scaffold materials, the capacity for alveolar bone and soft tissue remodeling on the material surface represents a pivotal factor in the effective application of biomaterials.[33] In this study, mouse pre-osteoblasts (MC3T3-E1) and a human periodontal fibroblast (HGF-1) model were utilized to simulate cellular processes associated with bone and connective tissue biology respectively. Fig. 9 shows the proliferation of MC3T3-E1 and HGF-1 cells cultured on different materials. All results indicate that the number of cells on the material surfaces increased with extended culture time, suggesting that none of the experimental groups exhibited significant cytotoxicity. As shown in Fig. 9A, there were no significant differences in early osteoblast proliferation among all the materials tested. However, on days 4 and 7, the proliferation ability of osteoblasts on the immersed CNF materials decreased compared to both the negative control group cultured on 24 well plates and the positive control groups comprising GC membranes and pure titanium. This reduction may be attributed to morphological alterations caused by the swelling of CNF materials in liquid, which could affect cell proliferation; however, this hypothesis requires further experimental verification.

Since HGF-1 cells are primary cells, their proliferative capacity significantly differs from that of immortalized cell

lines. In Fig. 9B, all experimental groups exhibit decreased overall OD values at equivalent time points compared to Fig. 9A. Notably, the GC membrane group demonstrates significantly higher cell proliferation among all groups, especially on day 7. This phenomenon contrasts with the observations in Fig. 9A and may be attributed to the inherent lack of differentiation tendency in HGF-1 cells, which could further amplify the proliferation-promoting effect of the GC membrane. The trends observed in the other groups are consistent with those noted in Fig. 9A.

Moreover, in Fig. 9, CNF-0.2 exhibited better biocompatibility compared to CNF-1, which may also relate to the surface morphology of the material. In previous studies, the surface contains tiny bumps and intertwined fibers, which can provide a barrier for soft tissues and enhance the growth of osteoblasts. And also shown that this rough surface structure is more conducive to cell proliferation.[34] In this study, higher roughness and a more prominent fibrous structure also facilitate cell proliferation.[35,36]

ALP is an early marker of osteoblast differentiation.[37] As shown in Fig. 10, the ALP activity of each group gradually increased over time. On the 21st day, the activity of CNF-0.2 and CNF-1 was lower than that of GC Membrane but higher than that of titanium. This indicates that CNF are also suitable as important materials for bone tissue engineering and regenerative medicine. Furthermore, CNF-0.2 demonstrated a better ability to promote osteogenic differentiation compared to CNF-1.

In this study, we proposed a novel dental biomaterial. As a scaffold material, CNF has better biocompatibility, hydrophilicity, and slightly degradability compared to titanium, but their mechanical properties still need improvement. On the other hand, as a membrane material, CNF has better mechanical properties than GC Membrane, but their degradability and biocompatibility still require enhancement. Despite these issues, CNF has demonstrated the potential to become a novel dental biomaterial. This study represents only a preliminary attempt to use CNF as dental biomaterials. While antimicrobial functionality represents a critical requirement for clinical dental materials, the unmodified CNF investigated in this preliminary study inherently lacks bactericidal activity due to its native polysaccharide structure.[38] This fundamental characteristic precluded antimicrobial assessment in the current experimental framework. The present work focuses on establishing the baseline material properties as a foundation for future functionalization strategies. Notably, CNF's unique chemical structure, with three reactive hydroxyl groups per anhydroglucose unit (C_6—OH, C_2—OH, and C_3—OH), offers versatile sites for covalent modification.[39] In future research, because of each glucose unit in cellulose contains three hydroxyl groups, providing chemical reactivity that facilitates the introduction of functional groups, we plan to utilize the abundant hydroxyl groups in CNF for various modification methods, aiming to apply them as potentially different dental biomaterials.[40] Additionally, controlling material deformation in operational environments will be a key focus of future research.

In conclusion, we report on CNF as a novel multifunctional potential dental biomaterial. Although unmodified cellulose nanofiber (CNF) materials exhibit certain limitations compared to commercial products, this work demonstrated significant research potential and prospects of CNF in dental applications. Moreover, their plant-derived origin provides a foundation for environmental friendliness and sustainable development.

Declaration of competing interest

The authors have no conflicts of interest relevant to this article.

Acknowledgments

This study was supported by the JST SPRING, Japan (grant number: JPMJSP2114).

References

1. Bottino MC, Thomas V, Schmidt G, et al. Recent advances in the development of GTR/GBR membranes for periodontal regeneration—a materials perspective. *Dent Mater* 2012;28:703—21.
2. Gotfredsen K, Nimb L, Hjørting-Hansen E. Immediate implant placement using a biodegradable barrier, polyhydroxybutyrate-hydroxyvalerate reinforced with polyglactin 910. An experimental study in dogs. *Clin Oral Implants Res* 1994;5:83—91.
3. Gottlow J. Guided tissue regeneration using bioresorbable and non-resorbable devices: initial healing and long-term results. *J Periodontol* 1993;64:1157—65.
4. Zitzmann NU, Naef R, Schärer P. Resorbable versus non-resorbable membranes in combination with Bio-Oss for guided bone regeneration. *Int J Oral Maxillofac Implants* 1997;12:844—52.
5. Hämmerle CH, Lang NP. Single stage surgery combining transmucosal implant placement with guided bone regeneration and bioresorbable materials. *Clin Oral Implants Res* 2001;12:9—18.
6. Wang J, Wang L, Zhou Z, et al. Biodegradable polymer membranes applied in guided bone/tissue regeneration: a review. *Polymers* 2016;8:115.
7. Abe GL, Sasaki JI, Tsuboi R, Kohno T, Kitagawa H, Imazato S. Poly (lactic acid/caprolactone) bilayer membrane achieves bone regeneration through a prolonged barrier function. *J Biomed Mater Res B Appl Biomater* 2024;112:35365.
8. Rothamel D, Schwarz F, Sager M, Herten M, Sculean A, Becker J. Biodegradation of differently cross-linked collagen membranes: an experimental study in the rat. *Clin Oral Implants Res* 2005;16:369—78.
9. Aprile P, Letourneur D, Simon-Yarza T. Membranes for guided bone regeneration: a road from bench to bedside. *Adv Healthcare Mater* 2020;9:2000707.
10. Distefano F, Pasta S, Epasto G. Titanium lattice structures produced via additive manufacturing for a bone scaffold: a review. *J Funct Biomater* 2023;14:125.
11. Briguglio F, Falcomatà D, Marconcini S, Fiorillo L, Briguglio R, Farronato D. The use of titanium mesh in guided bone regeneration: a systematic review. *Int J Dent* 2019;2019:9065423.
12. Gutta R, Baker RA, Bartolucci AA, Louis PJ. Barrier membranes used for ridge augmentation: is there an optimal pore size? *J Oral Maxillofac Surg* 2009;67:1218—25.
13. Alavi SE, Gholami M, Shahmabadi HE, Reher P. Resorbable GBR scaffolds in oral and maxillofacial tissue engineering: design, fabrication, and applications. *J Clin Med* 2023;12:6962.

14. Li Z, Du T, Gao C, et al. In-situ mineralized homogeneous collagen-based scaffolds for potential guided bone regeneration. *Biofabrication* 2022;14:045016.
15. Yang G, Liu H, Cui Y, et al. Bioinspired membrane provides periosteum-mimetic microenvironment for accelerating vascularized bone regeneration. *Biomaterials* 2021;268:120561.
16. Xia D, Yang F, Zheng Y, Liu Y, Zhou Y. Research status of biodegradable metals designed for oral and maxillofacial applications: a review. *Bioact Mater* 2021;6:4186—208.
17. Garot C, Bettega G, Picart C. Additive manufacturing of material scaffolds for bone regeneration: toward application in the clinics. *Adv Funct Mater* 2021;31:2006967.
18. Cheng BC, Jaffee S, Averick S, Swink I, Horvath S, Zhukauskas R. A comparative study of three biomaterials in an ovine bone defect model. *Spine J* 2020;20:457—64.
19. Amaral Valladão CA, Freitas Monteiro M, Joly JC. Guided bone regeneration in staged vertical and horizontal bone augmentation using platelet-rich fibrin associated with bone grafts: a retrospective clinical study. *Int J Oral Maxillofac Implants* 2020;6:1—10.
20. Bhat A, Khan I, Usmani MA, Umapathi R, Al-Kindy SM. Cellulose an ageless renewable green nanomaterial for medical applications: an overview of ionic liquids in extraction, separation and dissolution of cellulose. *Int J Biol Macromol* 2019;129:750—77.
21. Filipova I, Serra F, Tarres Q, Mutje P, Delgado-Aguilar M. Oxidative treatments for cellulose nanofibers production: a comparative study between TEMPO-mediated and ammonium persulfate oxidation. *Cellulose* 2020;27:10671—88.
22. Isogai A. Wood nanocelluloses: fundamentals and applications as new bio-based nanomaterials. *J Wood Sci* 2013;59:449—59.
23. Nishino T, Matsuda I, Hirao K. All-cellulose composite. *Macromolecules* 2004;37:7683—7.
24. Zou W, Hong G, Yamazaki Y, et al. Use of cellulose nanofibers as a denture immersing solution. *Dent Mater J* 2020;39:80—8.
25. Bahadoran Baghbadorani N, Behzad T, Karimi Darvanjooghi MH, Etesami N. Modelling of water absorption kinetics and biocompatibility study of synthesized cellulose nanofiber-assisted starch-graft-poly (acrylic acid) hydrogel nanocomposites. *Cellulose* 2020;27:9927—45.
26. Rol F, Belgacem MN, Gandini A, Bras J. Recent advances in surface-modified cellulose nanofibrils. *Prog Polym Sci* 2019;88:241—64.
27. Arima Y, Iwata H. Effect of wettability and surface functional groups on protein adsorption and cell adhesion using well-defined mixed self-assembled monolayers. *Biomaterials* 2007;28:3074—82.
28. Prasadh S, Wong RCW. Unraveling the mechanical strength of biomaterials used as a bone scaffold in oral and maxillofacial defects. *Oral Sci Int* 2018;15:48—55.
29. Yang Z, Wu C, Shi H, et al. Advances in barrier membranes for guided bone regeneration techniques. *Front Bioeng Biotechnol* 2022;10:921576.
30. Okahisa Y, Furukawa Y, Ishimoto K, Narita C, Intharapichai K, Ohara H. Comparison of cellulose nanofiber properties produced from different parts of the oil palm tree. *Carbohydr Polym* 2018;198:313—9.
31. Takata T, Miyauchi M, Wang HL. Migration of osteoblastic cells on various guided bone regeneration membranes. *Clin Oral Implants Res* 2001;12:332—8.
32. Vogel V, Sheetz M. Local force and geometry sensing regulate cell functions. *Nat Rev Mol Cell Biol* 2006;7:265—75.
33. MacBeth N, Trullenque-Eriksson A, Donos N, Mardas N. Hard and soft tissue changes following alveolar ridge preservation: a systematic review. *Clin Oral Implants Res* 2017;28:982—1004.
34. Rupp F, Liang L, Geis-Gerstorfer J, Scheideler L, Hüttig F. Surface characteristics of dental implants: a review. *Dent Mater* 2018;34:40—57.
35. Mu M, Liu S, DeFlorio W, et al. Influence of surface roughness, nanostructure, and wetting on bacterial adhesion. *Langmuir* 2023;39:5426—39.
36. Monteiro N, Fangueiro J, Reis R, Neves N. Replication of natural surface topographies to generate advanced cell culture substrates. *Bioact Mater* 2023;28:337—47.
37. Aubin J, Liu F, Malaval L, Gupta A. Osteoblast and chondroblast differentiation. *Bone* 1995;17:S77—83.
38. Rezaei A, Nasirpour A, Fathi M. Application of cellulosic nanofibers in food science using electrospinning and its potential risk. *Compr Rev Food Sci Food Saf* 2015;14:269—84.
39. Klemm D, Heublein B, Fink HP, Bohn A. Cellulose: fascinating biopolymer and sustainable raw material. *Angew Chem Int Ed Engl* 2005;44:3358—93.
40. Zhang C, Mo J, Fu Q, Liu Y, Wang S, Nie S. Wood-cellulose-fiber-based functional materials for triboelectric nanogenerators. *Nano Energy* 2021;81:105637.